Control of a flexible beam actuated by macro-fiber composite patches: I. Modeling and feedforward trajectory control

authored by **J. Schröck, T. Meurer, and A. Kugi**

and published in *Smart Materials and Structures*.

Contact:

Automation and Control Institute (ACIN)
Vienna University of Technology
Gusshausstrasse 27-29/E376
1040 Vienna, Austria

Internet: www.acin.tuwien.ac.at
E-mail: office@acin.tuwien.ac.at
Phone: +43 1 58801 37601
Fax: +43 1 58801 37699

Control of a flexible beam actuated by macro-fiber composite patches - Part I: Modelling and feedforward trajectory control

J. Schröck, T. Meurer, A. Kugi

Automation & Control Institute, Gußhausstr. 27-29, 1040 Vienna, Austria

E-mail: schroeck@acin.tuwien.ac.at

Abstract. This paper considers a systematic approach for motion planning and feedforward control design for a flexible cantilever actuated by piezoelectric macro-fiber composite (MFC) patches. For accurate feedforward tracking control, special attention has to be paid to the inherent nonlinear hysteresis and creep behavior of these actuators. In order to account for these effects an appropriate compensator is applied which allows to perform the tracking controller design on the basis of a linear infinite-dimensional model. A detailed analysis of the nonlinear actuator behavior as well as the compensator design and the overall experimental validation is presented in the companion paper [1]. The governing equations of motion of the hysteresis and creep compensated cantilever are determined by means of the extended Hamilton's principle. This allows to consider the influence of the bonded patch actuators on the mechanical properties of the underlying beam structure in a straightforward manner and results in a model with spatially varying system parameters. For the solution of the motion planning and feedforward control problem a flatness-based methodology is proposed. In a first step, the infinite-dimensional system of the MFC-actuated flexible cantilever is approximated by a finite-dimensional model, where all system variables, i.e. the states, input, and output, can be parametrized in terms of a so-called flat output. In a second step, it is shown by numerical simulations that these parametrizations converge with increasing system order of the finite-dimensional model such that the feedforward control input can be directly calculated in order to realize prescribed output trajectories.

Submitted to: *Smart Materials and Structures*

Post-print version of the article: J. Schröck, T. Meurer, and A. Kugi, "Control of a flexible beam actuated by macro-fiber composite patches: I. Modeling and feedforward trajectory control", *Smart Materials and Structures*, vol. 20, no. 015015, pp. 1–7, 2011. DOI: 10.1088/0964-1726/20/1/015015

1. Introduction

In the field of control of flexible structures special interest is dedicated to mechanical elements like beams and plates with integrated active materials, which endow the structures with distributed sensing and actuating capabilities [2], [3]. A very common realization of so-called smart structures uses piezoelectric patches that are bonded or embedded in the underlying carrier layer. The direct and indirect piezoelectric effect are thereby exploited to design appropriate sensing and actuating elements. The classical key example dealing with in-domain actuation and distributed sensing is vibration suppression [4]. Another application area is the shaping of flexible structures in order to realize adaptive elements. Here, in general two problems have to be distinguished. In the so-called static or dynamic shape control, the undeformed or respectively the initial state of the structure is preserved in view of static or dynamic loadings, see, e.g., [5] for a comprehensive overview. On the other hand, the active dynamical shape adaption of a flexible structure along prescribed trajectories by applying appropriate designed input signals to the actuators provides new and particularly promising applications. For example the shaping of an adaptive wing structure is shown in [6], where motion planning and feedforward control design are combined with results from optimal actuator placement to achieve a desired dynamical shape modification of a piezo-actuated cantilever plate.

Flexible structures are certainly described by partial differential equations (PDEs) and are thus infinite-dimensional systems. In strong contrast to the results on the stabilization problem, see, e.g., [7], only few analytical approaches exist to systematically solve the motion planning problem for infinite-dimensional systems. For finite-dimensional systems differential flatness [8] is a very well established tool in this context. Roughly speaking, differential flatness denotes the ability to parametrize all system states and inputs by a so-called flat output and its time-derivatives up to a certain problem-dependent order. This parametrization also corresponds to the determination of an inverse system representation in terms of the flat output. In the last years this concept has been successfully extended to certain classes of infinite-dimensional systems [9], [10], [11], [12], where the system inversion is performed with respect to the governing PDEs in order to retain the inherently infinite-dimensional system structure. In the field of flexible structures examples include Euler-Bernoulli beam models [13], [14], [15], [16], Timoshenko beam models [17], [18] and Kirchhoff plate models [6], [19]. In general, two different control approaches can be distinguished, namely boundary control and spatially distributed in-domain control. While boundary control is a widely studied topic in the literature there are only few contributions concerning in-domain control.

In the following, a flatness based approach is presented for motion planning and feedforward tracking control design for the example of a flexible beam with piezoelectric in-domain actuation. The beam consists of a flexible lightweight carrier layer and two piezoelectric patches, which are bonded symmetrically to the front and the back side of the beam, see figure 1. By applying voltage signals with opposite signs to the actuators,

Post-print version of the article: J. Schröck, T. Meurer, and A. Kugi, "Control of a flexible beam actuated by macro-fiber composite patches: I. Modeling and feedforward trajectory control", *Smart Materials and Structures*, vol. 20, no. 015015, pp. 1–7, 2011. DOI: 10.1088/0964-1726/20/1/015015
The content of this post-print version is identical to the published paper but without the publisher's final layout or copy editing.

bending strains are induced such that a deflection of the beam tip can be achieved. In this contribution the realization of high-speed point-to-point beam tip motions along prescribed trajectories is considered by exploiting the distributed parameter description of the beam for the solution of the motion planning and feedforward control problem. Additionally, the spatial distributions of the piezoelectric patches induce local stiffening in the structure. In order to achieve a high accuracy in the feedforward tracking control performance it is necessary to include these local effects in the distributed-parameter model. Finally, the consideration of viscous and Kelvin-Voigt damping completes the model, which is represented by a linear PDE with linear boundary conditions.

For the experimental validation of the proposed motion planning and feedforward control approach the application of macro-fiber composite (MFC) patches is an excellent choice for the actuation of flexible structures. In contrast to the very brittle nature of monolithic PZT (lead zirconate titanate) patches MFCs are composed of rectangular piezoelectric fibers embedded in an epoxy matrix and covered by interdigitated electrodes and thus result in very flexible patches. Additionally, the large input voltage range $[-500, +1500]$ V together with a larger electromechanical coupling coefficient compared to conventional PZT patches allow for higher actuation forces and larger displacements [20]. Similar to PZT patches and other active materials, like magneto- and electrostrictive materials and shape memory alloys, MFC actuators intrinsicly show hysteresis and creep effects. However, it can be shown that the MFC-actuated beam can be represented by a Hammerstein-like model consisting of a serial connection of the nonlinear hysteretic and creep model and a linear infinite-dimensional beam model. Since the detailed analysis of the nonlinear actuator behavior, which is necessary to clarify the compensator design, is beyond the scope of this paper the hysteresis and creep compensator and the overall experimental validation is presented in the companion paper [1]. There also experimental results for the realization of highly dynamic trajectories of the beam's tip deflection are presented, which demonstrate the applicability of the feedforward tracking control proposed in this contribution.

The paper is organized as follows: In Section 2, the governing equations of motion are derived for the MFC-actuated cantilever beam by means of an energy-based modeling approach using the extended Hamilton's principle. With this, the variational formulation is introduced, which can be efficiently utilized to determine the spectral representation of the equations of motion in Section 3. Based on this formulation the flatness-based motion planning and feedforward control design is presented in Section 4, which is validated by simulation in Section 5.

2. Energy-based modeling

In the following, the equations of motion are derived for the transverse deflection $w(x^1, t)$ in the x^3-direction of the cantilevered rectangular flexible beam as shown in figure 1. The beam is clamped at the position $x^1 = 0$ and free at the opposing end $x^1 = L$. The overall beam structure consists of a carrier layer (index c) and an MFC patch pair

Post-print version of the article: J. Schröck, T. Meurer, and A. Kugi, "Control of a flexible beam actuated by macro-fiber composite patches: I. Modeling and feedforward trajectory control", *Smart Materials and Structures*, vol. 20, no. 015015, pp. 1–7, 2011. DOI: 10.1088/0964-1726/20/1/015015
The content of this post-print version is identical to the published paper but without the publisher's final layout or copy editing.

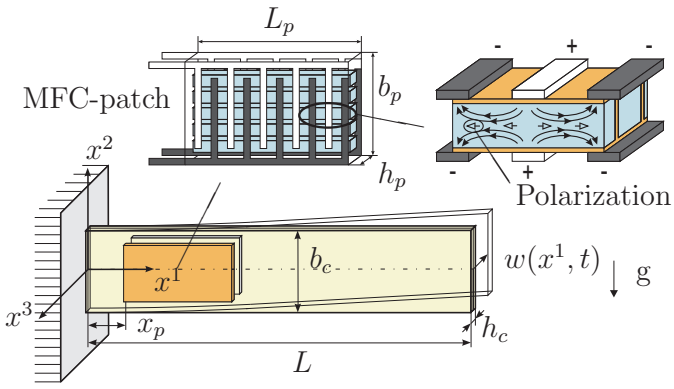

Figure 1. Schematics of the considered flexible beam actuated by one pair of MFC patches.

(index p) with two symmetrically placed actuators, one on the front side and one on the back side of the beam, respectively. The placement of the patch pair on the carrier layer is specified by the spatial actuator characteristics

$$\Omega(x^1) = \big[h(x^1 - x_p) - h(x^1 - x_p - L_p)\big] \tag{1}$$

with the Heaviside function $h(\cdot)$. For modeling purposes the rotational inertia of the beam structure as well as the adhesive layers between the patches and the carrier layer are neglected. The deflection of the beam is restricted to a pure bending motion, i.e. 1-dimensional motion in x^3-direction, by the application of an asymmetric voltage supply to the MFC patch pair. Therefor, the voltage applied to the patch on the front side of the beam $\overline{u}^{fs}(t)$ and the voltage applied to the patch on the back side of the beam $\overline{u}^{bs}(t)$ are given by

$$\overline{u}^{fs}(t) = u_0 + u(t) \text{ and } \overline{u}^{bs}(t) = u_0 - u(t), \tag{2}$$

respectively. Here, the constant supply voltage $u_0 = (u_{max} + u_{min})/2$ is used to enable a balanced voltage supply $u(t) \in [-\frac{u_{max}+|u_{min}|}{2}, +\frac{u_{max}+|u_{min}|}{2}]$, whereas $u_{min} = -500$ V and $u_{max} = 1500$ V are the actuator specific minimal and maximal supply voltages. Additionally, in the considered configuration the gravitational field in negative x^2-direction does not effect the beam motion, whereas in general gravitational effects can be easily included into the mathematical model.

2.1. Equations of motion

The governing equations of motion are derived by applying the extended Hamilton's principle, i.e.

$$\int_{t_0}^{t_e} [\delta T - \delta V + \delta N] \mathrm{d}t = 0, \tag{3}$$

where δ denotes the variational operator and $T = T_c + T_p$, $V = V_c + V_p$ represent the kinetic and the potential energy stored in the carrier layer and the MFC patch pair, respectively. The virtual work of non-conservative forces due to damping is summarized

Post-print version of the article: J. Schröck, T. Meurer, and A. Kugi, "Control of a flexible beam actuated by macro-fiber composite patches: I. Modeling and feedforward trajectory control", *Smart Materials and Structures*, vol. 20, no. 015015, pp. 1–7, 2011. DOI: 10.1088/0964-1726/20/1/015015
The content of this post-print version is identical to the published paper but without the publisher's final layout or copy editing.

in the term $N = N_c + N_p$. In the geometric linearized scenario the longitudinal strain ϵ_{11} is related to the bending deflection $w(x^1, t)$ by the Euler-Bernoulli assumption in the form $\epsilon_{11} = -x^3 \partial^2_{x^1} w$. Thus the potential energy of the carrier layer due to pure bending is given by

$$V_c = \tfrac{1}{2}\Lambda_c \int_0^L (\partial^2_{x^1} w)^2 \mathrm{d}x^1, \tag{4}$$

where $\Lambda_c = Y_c I_c$ with Young's modulus Y_c and the moment of inertia $I_c = h_c^3 b_c/12$. The kinetic energies of the carrier and the MFC patch pair read as

$$T_c = \tfrac{A_c \rho_c}{2} \int_0^L (\partial_t w)^2 \mathrm{d}x^1, \qquad T_p = 2\tfrac{A_p \rho_p}{2} \int_0^L \Omega(x) (\partial_t w)^2 \mathrm{d}x^1 \tag{5}$$

with $A_c = b_c h_c$, $A_p = b_p h_p$ and ρ_c, ρ_p denoting the respective cross section and mass density.

The complex structure of the MFC patch actuators (cf. figure 1) is modeled by a homogenized orthotropic material with appropriate material parameters provided by the distributor [21]. Hence the potential energy of a single MFC-patch is given in the form

$$V_p^s = \int_V \left(\sigma^{ij}\epsilon_{ij} + E_i D^i\right) \mathrm{d}x^1 \mathrm{d}x^2 \mathrm{d}x^3, \tag{6}$$

with the components of the mechanical stress tensor σ^{ij}, the components of the strain tensor ϵ_{ij}, the components of the electric field E_i, the components of the electric flux density D^i, $i, j = 1, 2, 3$, and V as the volume of the MFC-patch. As pointed out in the introduction, for the modeling of the beam structure a linear constitutive relation is considered under the assumption that all actuator nonlinearities are canceled out by means of an appropriate hysteresis and creep compensator. A detailed analysis of the specific hysteresis and creep behavior as well as the derivation of the compensator is presented in the companion paper [1]. The additional assumption of an uniaxial state of stress and the approximation of the electric field between the interdigitated electrodes in the MFC-patch by an exclusive homogeneous field component E_1 with simultaneously vanishing electric flux density components $D^2 = D^3 = 0$ yields the following simplified linear constitutive relation

$$\begin{aligned} \sigma^{11} &= c^{1111}\epsilon_{11} - h_1^{11} D^1, \\ E_1 &= -h_1^{11}\epsilon_{11} + \beta_{11} D^1, \end{aligned} \tag{7}$$

see, e.g., [22]. Here, σ^{11} and ϵ_{11} denote the longitudinal mechanical stress and strain component, respectively, and c^{1111}, h_1^{11} and β_{11} indicate material parameters. With these constitutive equations the potential energy (6) evaluates to

$$V_p^s = \frac{1}{2} \int_V \left(c^{1111} \left(\epsilon_{11}\right)^2 - 2 h_1^{11} D^1 \epsilon_{11} + \beta_{11} \left(D^1\right)^2 \right) \mathrm{d}x^1 \mathrm{d}x^2 \mathrm{d}x^3. \tag{8}$$

Assuming that the self-generated electric field due to the direct piezoelectric effect $-h_1^{11}\epsilon_{11}$ in (7) is insignificant compared to the electric field component E_1, the integration along E_1 between two neighboring electrodes with distance e_s leads to

$$\int_{x_e}^{x_e + e_s} E_1 \mathrm{d}x^1 = \beta_{11} D^1 e_s = \overline{u}, \tag{9}$$

Post-print version of the article: J. Schröck, T. Meurer, and A. Kugi, "Control of a flexible beam actuated by macro-fiber composite patches: I. Modeling and feedforward trajectory control", *Smart Materials and Structures*, vol. 20, no. 015015, pp. 1–7, 2011. DOI: 10.1088/0964-1726/20/1/015015

where $\overline{u}(t)$ denotes the voltage applied to the actuator. Considering (9) with the appropriate asymmetric voltage supply and evaluating the specific volume integrals of the potential energy (8) for the patch on the front and back side of the beam the potential energy of the MFC patch pair evaluates to

$$V_p = \int_0^L \Omega(x^1) \left(\Lambda_p(\partial^2_{x^1} w)^2 + 2u\Gamma_p \partial^2_{x^1} w\right) \mathrm{d}x^1, \tag{10}$$

where $\Lambda_p = c_p^{1111} b_p([h_c/2 + h_p]^3 - h_c^3/8)/3$ and $\Gamma_p = A_p(h_c + h_p)h_1^{11}/(2\beta_{11}e_s)$. Note that the term $\beta_{11}\left(D^1\right)^2$ in (8) is neglected since by the assumption of ideal voltage sources this term vanishes in the following variational formulation.

In order to include damping into the analysis the variational derivatives of the virtual work of the nonconservative damping forces N_c and N_p originating from the carrier layer and the MFC patch pair are considered in the form

$$\delta N_c = -\int_0^L (\gamma_c^e \partial_t w \delta w + \gamma_c^i \partial_t \partial^2_{x^1} w \delta(\partial^2_{x^1} w))\mathrm{d}x^1, \tag{11}$$

$$\delta N_p = -2\int_0^L \Omega(x^1)(\gamma_p^e \partial_t w \delta w + \gamma_p^i \partial_t \partial^2_{x^1} w \delta(\partial^2_{x^1} w))\mathrm{d}x^1. \tag{12}$$

Thereby, the parameters γ_c^e and γ_p^e refer to viscous (external) damping while γ_c^i and γ_p^i represent Kelvin-Voigt (internal) damping.

The equations of motion for the MFC-actuated beam can be directly determined by evaluating (3) together with the fundamental lemma of variational calculus, which yields

$$\begin{aligned} &\mu(x^1)\partial_t^2 w + \gamma^e(x^1)\partial_t w + \partial^2_{x^1}\left(\Lambda(x^1)\partial^2_{x^1} w + \gamma^i(x^1)\partial_t \partial^2_{x^1} w\right) \\ &= -2u\Gamma_p \partial^2_{x^1}\Omega(x^1), \end{aligned} \tag{13}$$

where $\mu(x^1) = A_c\rho_c + 2A_p\rho_p\Omega(x^1)$, $\Lambda(x^1) = \Lambda_c + 2\Lambda_p\Omega(x^1)$, $\gamma^e(x^1) = \gamma_c^e + 2\gamma_p^e\Omega(x^1)$, and $\gamma^i(x^1) = \gamma_c^i + 2\gamma_p^i\Omega(x^1)$. The respective boundary conditions (BCs) at the clamped end follow as

$$w = 0,\ \partial_{x^1} w = 0, \qquad \text{for} \quad x^1 = 0 \tag{14}$$

while at the free end

$$\left.\begin{aligned} \Lambda_c \partial^2_{x^1} w + \gamma_c^i \partial_t \partial^2_{x^1} w = 0, \\ \Lambda_c \partial^3_{x^1} w + \gamma_c^i \partial_t \partial^3_{x^1} w = 0, \end{aligned}\right\} \qquad \text{for} \quad x^1 = L. \tag{15}$$

For the sake of simplicity, zero initial conditions (ICs) are assumed, i.e. $w(x^1, 0) = w_0(x^1) \equiv 0$, $\partial_t w(x^1, 0) = w_1(x^1) \equiv 0$ $x^1 \in [0, L]$, which, for non-zero stationary ICs can be obtained by a simple state transformation.

3. Variational form and modal representation

Clearly, the spatial distribution of the patch actuators leads to local variations of inertia, stiffness and damping resulting in derivatives of the Heaviside function, which is included in the definition of $\Omega(x^1)$. In order to overcome the necessity to consider distributional solutions the weak or variational form of (13)-(15) is subsequently considered, see, e.g., [3], [23].

Post-print version of the article: J. Schröck, T. Meurer, and A. Kugi, "Control of a flexible beam actuated by macro-fiber composite patches: I. Modeling and feedforward trajectory control", *Smart Materials and Structures*, vol. 20, no. 015015, pp. 1–7, 2011. DOI: 10.1088/0964-1726/20/1/015015
The content of this post-print version is identical to the published paper but without the publisher's final layout or copy editing.

3.1. Variational form

Let $\mathcal{V} = H_0^2(0,L) = \{w \in H^2 | w = \partial_{x^1} w = 0 \text{ on } x^1 = 0\}$ and $\mathcal{H} = L^2(0,L)$ and observe that these spaces form a Gelfand triple $\mathcal{V} \subset \mathcal{H} = \mathcal{H}' \subset \mathcal{V}'$, where $\mathcal{H}$, the so-called pivot space, can be identified with its dual $\mathcal{H}'$ by the Riesz representation theorem. By means of the inner product on $\mathcal{H}$, which is defined by $\langle \phi, \theta \rangle_{\mathcal{H}} = \int_0^L \phi\theta \mathrm{d}x^1$, it follows that the weak form of (13)-(15) can be also represented by

$$\left\langle \mu(x^1)\partial_t^2 w, \xi \right\rangle_{\mathcal{H}} + \sigma_1(w,\xi) + \sigma_2(w,\xi) = -\left\langle 2u\Gamma_p \Omega(x^1), \partial_{x^1}^2 \xi \right\rangle_{\mathcal{H}} \tag{16}$$

with an appropriate test function $\xi(x^1) \in \mathcal{V}$. It can be easily verified that $\sigma_{1,2} : \mathcal{V} \times \mathcal{V} \to \mathbb{R}$, defined as

$$\sigma_1(w,\xi) = \int_0^L \Lambda(x^1)\partial_{x^1}^2 w \partial_{x^1}^2 \xi \mathrm{d}x^1, \tag{17}$$

$$\sigma_2(w,\xi) = \int_0^L (\gamma^e(x^1) w\xi + \gamma^i(x)\partial_{x^1}^2 w \partial_{x^1}^2 \xi)\mathrm{d}x^1, \tag{18}$$

represent symmetric, bounded, and coerziv sesquilinear forms such that the Lax-Milgram theorem implies the existence and uniqueness of a solution $w(x^1,t)$ with the regularity properties $w \in L^2(0,T;\mathcal{V})$, $\partial_t w \in L^2(0,T;\mathcal{H})$, and $\partial_t^2 w \in L^2(0,T;\mathcal{V}')$ can be ensured [3], [23].
Based on the variational form (16), a modal representation is determined in the following, which serves as a basis for the subsequent solution of the motion planning and feedforward control problem.

3.2. Modal representation

Without requiring any additional regularity on the parameters $\mu(x^1)$, $\Lambda(x^1)$, $\gamma^e(x^1)$, and $\gamma^i(x^1)$ the modal representation of the MFC-actuated cantilever beam can be efficiently determined by utilizing the variational form (16). By replacing the displacement $w(x^1,t)$ with the finite-dimensional approximation

$$w(x^1,t) = \sum_{k=1}^{n} q_k(t)\phi_k(x^1), \tag{19}$$

the evaluation of the variational formulation with the test function $\xi(x^1) = \phi_k(x^1) \in \mathcal{V}$ for each $k \in \mathbb{N}$ transfers the distributed-parameter system into a finite-dimensional linear system of coupled second order ordinary differential equations (ODEs), i.e.

$$\begin{aligned} &M\partial_t^2 \mathbf{q} + C\partial_t \mathbf{q} + K\mathbf{q} = \mathbf{b}u, \\ &y = \mathbf{c}^T \mathbf{q} \end{aligned} \tag{20}$$

with $\mathbf{q}(t) = [q_1(t), q_2(t), ..., q_n(t)]^T$ and the symmetric matrices $M = M_c + M_p \in \mathbb{R}^{n\times n}$, $C = C_c + C_p \in \mathbb{R}^{n\times n}$, $K = K_c + K_p \in \mathbb{R}^{n\times n}$, the input vector $\mathbf{b} \in \mathbb{R}^{n\times 1}$ and the output

Post-print version of the article: J. Schröck, T. Meurer, and A. Kugi, "Control of a flexible beam actuated by macro-fiber composite patches: I. Modeling and feedforward trajectory control", *Smart Materials and Structures*, vol. 20, no. 015015, pp. 1–7, 2011. DOI: 10.1088/0964-1726/20/1/015015
The content of this post-print version is identical to the published paper but without the publisher's final layout or copy editing.

vector $\mathbf{c}^T \in \mathbb{R}^{1\times n}$ determined by

$$\begin{aligned}
[M_c]_{k,l} &= A_c\rho_c \textstyle\int_0^L \phi_k\phi_l \mathrm{d}x^1, & [M_p]_{k,l} &= 2A_p\rho_p \textstyle\int_{x_p}^{x_p+L_p} \phi_k\phi_l \mathrm{d}x^1,\\
[C_c]_{k,l} &= \textstyle\int_0^L (\gamma_c^e\phi_k\phi_l + \gamma_c^i\partial^2_{x^1}\phi_k\partial^2_{x^1}\phi_l)\mathrm{d}x^1, & [C_p]_{k,l} &= 2\textstyle\int_{x_p}^{x_p+L_p} (\gamma_p^e\phi_k\phi_l + \gamma_p^i\partial^2_{x^1}\phi_k\partial^2_{x^1}\phi_l)\mathrm{d}x^1,\\
[K_c]_{k,l} &= \Lambda_c \textstyle\int_0^L \partial^2_{x^1}\phi_k\partial^2_{x^1}\phi_l \mathrm{d}x^1, & [K_p]_{k,l} &= 2\Lambda_p \textstyle\int_{x_p}^{x_p+L_p} \partial^2_{x^1}\phi_k\partial^2_{x^1}\phi_l \mathrm{d}x^1,\\
[b]_k &= -2\Gamma_p \textstyle\int_{x_p}^{x_p+L_p} \partial^2_{x^1}\phi_k \mathrm{d}x^1, & [c]_k &= \phi_k(L),
\end{aligned} \tag{21}$$

where the output of the system equals the beam's tip deflection, i.e. $y(t) = w(L,t)$. For the evaluation of (21), the basis functions $\phi_k(x^1)$ can be chosen as the eigenfunctions of an undamped cantilevered Euler-Bernoulli beam ($\partial^4_{x^1} w = \hat{\lambda} w$) since they form a complete basis of the space $\mathcal{V}$. In order to determine the modal representation in terms of the eigenmodes the eigenvalue problem for (20), i.e. $(M\lambda^2 + C\lambda + K)\psi = 0$, is considered. Due to the non-proportional damping, i.e. $\nexists \iota_1, \iota_2 \in \mathbb{R} : C = \iota_1 M + \iota_2 K$ it is convenient to re-write the system in the form of 1st order ODEs

$$\begin{aligned}
&\tilde{M}\partial_t\boldsymbol{\eta} + \tilde{K}\boldsymbol{\eta} = \tilde{\mathbf{b}}u,\\
&y = \tilde{\mathbf{c}}^T\boldsymbol{\eta}
\end{aligned} \tag{22}$$

with $\boldsymbol{\eta} = [\mathbf{q}^T, \partial_t\mathbf{q}^T]^T$, the symmetric matrices $\tilde{M} = \left[\begin{smallmatrix} C & M \\ M & 0 \end{smallmatrix}\right]$ and $\tilde{K} = \left[\begin{smallmatrix} K & 0 \\ 0 & -M \end{smallmatrix}\right]$ as well as the vectors $\tilde{\mathbf{b}} = [\mathbf{b}^T, \mathbf{0}^T]^T$ and $\tilde{\mathbf{c}} = [\mathbf{c}^T, \mathbf{0}^T]^T$. Based on this representation the generalized eigenvalue problem is given as

$$(\tilde{M}\lambda + \tilde{K})\boldsymbol{\theta} = 0, \tag{23}$$

with each eigenvector being composed according to $\boldsymbol{\theta} = [\boldsymbol{\psi}, \lambda\boldsymbol{\psi}]^T$. In case of the considered beam structure all eigenvalues arise in complex conjugate pairs $\lambda_j = \overline{\lambda}_{-j}$ together with the respective complex conjugate pairs of eigenvectors $\boldsymbol{\theta}_j = \overline{\boldsymbol{\theta}}_{-j}$ with $j \in Z_n$, $Z_n := \{-n, ..., n\} \setminus \{0\}$. Thereby, the ortho-normality conditions $\Theta^T\tilde{M}\Theta = I$ and $\Theta^T\tilde{K}\Theta = -\Xi$ are satisfied, where I represents the identity matrix and $\Xi = \mathrm{diag}\{\lambda_j\}$ with $j \in Z_n$ and $\Theta = [\boldsymbol{\theta}_{-n}, ..., \boldsymbol{\theta}_n]$ denotes the transformation matrix. Applying the coordinate transformation $\boldsymbol{\eta}(t) = \Theta\boldsymbol{\zeta}(t)$, (22) can be re-written as a decoupled set of 1st order ODEs with complex coefficients, i.e.

$$\partial_t\zeta_j - \lambda_j\zeta_j = \boldsymbol{\psi}_j^T\mathbf{b}u, \quad j \in Z_n \tag{24}$$

$$y = \sum_{j\in Z_n} \mathbf{c}^T\boldsymbol{\psi}_j\zeta_j. \tag{25}$$

with initial conditions $\zeta_j(0) = 0$, $j \in Z_n$. This modal representation serves as the basis for the subsequently proposed approach for motion planning and feedforward control design. From (19) it follows that the realization of an arbitrary trajectory for the beam's tip deflection requires the system to be modal (state) controllable [24]. Modal state controllable means that every mode $\zeta_j(t)$ can be influenced by the input $u(t)$. For the single input system (24), (25) this requires that the eigenvalues λ_j are mutually distinct and that the coefficients $\boldsymbol{\psi}_j^T\mathbf{b}$ are non-zero for all $j \in Z_n$.

Post-print version of the article: J. Schröck, T. Meurer, and A. Kugi, "Control of a flexible beam actuated by macro-fiber composite patches: I. Modeling and feedforward trajectory control", *Smart Materials and Structures*, vol. 20, no. 015015, pp. 1–7, 2011. DOI: 10.1088/0964-1726/20/1/015015
The content of this post-print version is identical to the published paper but without the publisher's final layout or copy editing.

4. Flatness-based motion planning and feedforward tracking control design

For finite-dimensional control systems the property of differential flatness implies that any system state and input can be parametrized by the so-called flat output and its time-derivatives up to a certain problem dependent order [8]. This concept can in principle be transferred to infinite-dimensional systems, where a so-called basic output is introduced corresponding to a flat output. However, there exist a number of different approaches, which result in the construction of a parametrizing function or flat output in order to represent the inverse system.
In a first step, a flatness-based parametrization of the modal states, the output given by the deflection of the beam's tip, and the input of the system is derived based on the finite-dimensional modal system representation. In the second step, it is shown by numerical investigations in Section 5 that these parametrizations converge for increasing number of approximation terms.

4.1. Flatness-based parametrization

Based on the decoupled system representation (24), (25) a flat or basic output $z(t)$ is systematically constructed. For this, the Laplace transform applied to (24) yields

$$\hat{\zeta}_j = \frac{\boldsymbol{\psi}_j^T \mathbf{b}}{s - \lambda_j} \hat{u}, \quad j \in Z_n, \tag{26}$$

where $\hat{\zeta}_j(s)$ and $\hat{u}(s)$ denote the Laplace transforms of $\zeta_j(t)$ and $u(t)$, respectively. By suitably expanding the resolvent $\frac{1}{s-\lambda_j}$, (26) can be reformulated in terms of the operators $D_\zeta^j(s)$ and $D_u(s)$ according to

$$\hat{\zeta}_j = \frac{D_\zeta^j(s)}{D_u(s)} \hat{u}, \quad j \in Z_n \tag{27}$$

with

$$D_\zeta^j(s) = -\alpha_j \prod_{\substack{k=1 \\ k \neq |j|}}^{n} \Big(1 - s\Big(\frac{1}{\lambda_k} + \frac{1}{\overline{\lambda}_k}\Big) + \frac{s^2}{\lambda_k \overline{\lambda}_k}\Big), \tag{28}$$

$$D_u(s) = \prod_{k=1}^{n} \Big(1 - s\Big(\frac{1}{\lambda_k} + \frac{1}{\overline{\lambda}_k}\Big) + \frac{s^2}{\lambda_k \overline{\lambda}_k}\Big), \tag{29}$$

where $\alpha_j = 1/\lambda_j \boldsymbol{\psi}_j^T \mathbf{b}(1 - s/\overline{\lambda}_j)$, $j \in Z_n$. The introduction of $\hat{z}(s) = \hat{u}(s)/D_u(s)$, results in an operational parametrization of the states $\hat{\zeta}_j(s)$, $j \in Z_n$, the input $\hat{u}(s)$, and the output $\hat{y}(s)$ of the system in terms of $\hat{z}(s)$, i.e.

$$\hat{\zeta}_j = D_\zeta^j(s)\hat{z}, \quad j \in Z_n, \tag{30}$$

$$\hat{u} = D_u(s)\hat{z}, \tag{31}$$

$$\hat{y} = \sum_{j \in Z_n} \mathbf{c}^T \boldsymbol{\psi}_j D_\zeta^j(s)\hat{z}. \tag{32}$$

Post-print version of the article: J. Schröck, T. Meurer, and A. Kugi, "Control of a flexible beam actuated by macro-fiber composite patches: I. Modeling and feedforward trajectory control", *Smart Materials and Structures*, vol. 20, no. 015015, pp. 1–7, 2011. DOI: 10.1088/0964-1726/20/1/015015
The content of this post-print version is identical to the published paper but without the publisher's final layout or copy editing.

This system representation can be easily transformed into the time domain due to the fact that s in the operational domain corresponds to the time differentiation in the time domain. Hence, all system variables can be parametrized by the function $z(t)$ and its time derivatives up to the order $2n$ according to the following relations

$$\zeta_j = (D_\zeta^j(s)z)|_{s^k=\frac{\mathrm{d}^k}{\mathrm{d}t^k},\ k=0,1,\ldots,2n-1} \tag{33}$$

$$u = (D_u(s)z)|_{s^k=\frac{\mathrm{d}^k}{\mathrm{d}t^k},\ k=0,1,\ldots,2n} \tag{34}$$

$$y = \sum_{j\in Z_n} \mathbf{c}^T \boldsymbol{\psi}_j (D_\zeta^j(s)z)|_{s^k=\frac{\mathrm{d}^k}{\mathrm{d}t^k},\ k=0,1,\ldots,2n-1.} \tag{35}$$

As a result $z(t)$ constitutes a flat or basic output of (24)-(25) or (20), respectively. The determined parametrization can be utilized for the design of a feedforward tracking controller by prescribing a smooth desired trajectory $t \mapsto z^d(t)$ for the flat output $z(t)$. For this, the evaluation of (34) requires that any admissible trajectory $z^d(t)$ is at least $2n$ times continuously differentiable, i.e. $z^d(t) \in C^{2n}(\mathbb{R}^+)$. It should be mentioned that due to the factor α_j in the operator $D_\zeta^j(s)$ the state trajectory $\zeta_j^d(t)$ is in general complex valued although $z_d(t)$ is real valued. However, the transformation $\boldsymbol{\eta} = [\mathbf{q}^T, \partial_t \mathbf{q}^T]^T = \Theta\boldsymbol{\zeta}$, where Θ involves the complex conjugated pairs of eigenvectors, guarantees real valued coefficients $q_k(t)$ in the series expansion for the deflection profile $w(x^1,t) = \sum_{k=1}^n q_k(t)\phi_k(x^1)$.

4.2. Motion planning

Based on the system parametrization in terms of the flat output $z(t)$ a very intuitive procedure can be found to solve the motion planning problem for the beam's tip deflection. As shown in Sec. 4.1 the assignment of an admissible trajectory $z^d(t)$ to the flat output $z(t)$ results in the output trajectory $y^d(t)$ determined by (35) with $z(t) = z^d(t)$. Hence, appropriate re-planning of $z^d(t)$ allows to realize a prescribed output trajectory $y^d(t)$. For the realization of a rest-to-rest motion from $y^d(0)$ to $y^d(T)$ along a prescribed transition path within the finite time interval $t \in [0,T]$ with specified transition time $T < \infty$, this problem can be solved by considering the corresponding relationship between the steady state values obtained from (35), i.e.

$$z^d(0) = \frac{-1}{\sum_{j\in Z_n} \frac{1}{\lambda_j} \mathbf{c}^T \boldsymbol{\psi}_j \boldsymbol{\psi}_j^T \mathbf{b}} y^d(0), \tag{36}$$

$$z^d(T) = \frac{-1}{\sum_{j\in Z_n} \frac{1}{\lambda_j} \mathbf{c}^T \boldsymbol{\psi}_j \boldsymbol{\psi}_j^T \mathbf{b}} y^d(T). \tag{37}$$

The choice of the transition function between the initial and final value $z^d(0)$ and $z^d(T)$ directly determines the actual output trajectory $y^d(t)$. Finally, the required feedforward control $u^d(t)$ for the realization of this output trajectory is computed by evaluating the input parametrization (34). Due to the fact that the resulting feedforward control

Post-print version of the article: J. Schröck, T. Meurer, and A. Kugi, "Control of a flexible beam actuated by macro-fiber composite patches: I. Modeling and feedforward trajectory control", *Smart Materials and Structures*, vol. 20, no. 015015, pp. 1–7, 2011. DOI: 10.1088/0964-1726/20/1/015015

is based on the finite-dimensional system (20) with n approximation terms, convergence has to be verified for the case $n \to \infty$. In this approach the convergence of the parametrizations (33)-(35) induced by the operators $D_u(s)$ and $D_\zeta^j(s)$ is directly related to the distributions of the eigenvalues. To the best knowledge of the authors, in case of stepwise varying material parameters no analytic solution for the eigenvalue problem corresponding to the infinite-dimensional system (13)-(15) exists in the literature. However, numerical simulations show a fast convergence of the parametrizations (33)-(35) with increasing number of approximation terms n, as will be presented in the next section.

5. Simulation and numerical convergence

The simulation scenario considered in this contribution refers to the experimental setup investigated in the companion paper [1]. The cantilever beam structure consists of a pre-impregnated glass fibre material of dimension $L = 0.22\,\mathrm{m}$, $b_c = 0.075\,\mathrm{m}$, and $h_c = 0.7 \times 10^{-3}\,\mathrm{m}$. On each side of the beam an MFC patch actuator (type $M8557P1$, see [21]) with an active area of dimension $L_p = 85 \times 10^{-3}\mathrm{m}$, $b_p = 57 \times 10^{-3}\mathrm{m}$, $h_p = 3 \times 10^{-4}\mathrm{m}$, and electrode spacing $e_s = 5 \times 10^{-4}\,\mathrm{m}$, is bonded symmetrically at a distance of $x_p = 32.5 \times 10^{-3}\mathrm{m}$ from the clamped edge (cf. figure 1). Additionally, the system parameters are identified according to $\gamma_c^e = 10^{-3}\,\mathrm{kg/(sm)}$, $\gamma_c^i = 5.1 \times 10^5\,\mathrm{kgm^3/s}$, $\gamma_p^e = 2.93\,\mathrm{kg/(sm)}$, $\gamma_p^i = 10^6\,\mathrm{kgm^3/s}$, $Y_c = 17.06 \times 10^9\,\mathrm{Pa}$, $c_p^{1111} = 31.97 \times 10^9\,\mathrm{Pa}$, $\rho_c = 1187.6\,\mathrm{kg/m^3}$, $\rho_p = 4761.4\,\mathrm{kg/m^3}$, and $a_1^{11}/\beta_{11} = 11.88\,\mathrm{As/m^2}$.
Numerical investigations with a varying number of elements n in the series expansion (19) illustrate the convergence of the state and input parametrizations (33), (34). For this, a rest-to-rest transition starting at $y^d(0) = 0\,\mathrm{m}$ to reach $y^d(T) = 0.01\,\mathrm{m}$ with $T = 75\,\mathrm{ms}$ is considered. The desired trajectory for the flat output $z^d(t)$ is prescribed by the transition function

$$z^d(t) = \begin{cases} z_0^d, & t < 0 \\ z_0^d + \frac{z_T^d}{2}\left(1 + \tanh\left(\frac{2\left(\frac{2t}{T}-1\right)}{\left(\frac{4t}{T}\left(1-\frac{t}{T}\right)\right)^\sigma}\right)\right), & t \in [0,T] \\ z_0^d + z_T^d, & t > T \end{cases} \tag{38}$$

where $\sigma = 1.1$ denotes the slope of the transition function, see figure 2 (a). In addition to the flat output trajectory $z^d(t)$, figure 2 illustrates the resulting feedforward control $u^d(t)$ and the output trajectory $y^d(t)$, whereas the signals are calculated for different numbers of approximation terms $n = 1, 10, 15, 20$. It can be seen that for the realization of the rest-to-rest motion within the transition time of $T = 75\,\mathrm{ms}$ the required voltage signal evolves in a rather non-trivial manner with alternating phases of acceleration and deceleration before reaching the final stationary value. With increasing n also the waviness of the voltage signal increases, which results from the fact that the higher approximation terms are related to eigenfunctions with higher eigenfrequencies. As shown in figure 2, the contributions of the higher order

Post-print version of the article: J. Schröck, T. Meurer, and A. Kugi, "Control of a flexible beam actuated by macro-fiber composite patches: I. Modeling and feedforward trajectory control", *Smart Materials and Structures*, vol. 20, no. 015015, pp. 1–7, 2011. DOI: 10.1088/0964-1726/20/1/015015
The content of this post-print version is identical to the published paper but without the publisher's final layout or copy editing.

modes decay rapidly such that the parametrizations (33)-(35) converge and the signals hardly change for $n > 20$. Nevertheless, a convergence analysis is required in order to verify that the parametrizations (33)-(35) obtain a meaningful limit as $n \to \infty$. For the case of a viscously damped cantilevered Euler-Bernoulli beam convergence of the parametrizations (33)-(35) is investigated in [25]. However, these results are based on continuously differentiable parameter functions $\mu(x^1), \Lambda(x^1) \in C^4(0, L)$ and $\gamma^i(x^1) \in C^1(0, L)$. In case of stepwise parameter functions, as investigated in this contribution, the convergence analysis is still an open question and subject to further research. Nevertheless, for implementation issues it is sufficient to consider a sufficiently large n in order to capture the essential dynamics of the system.

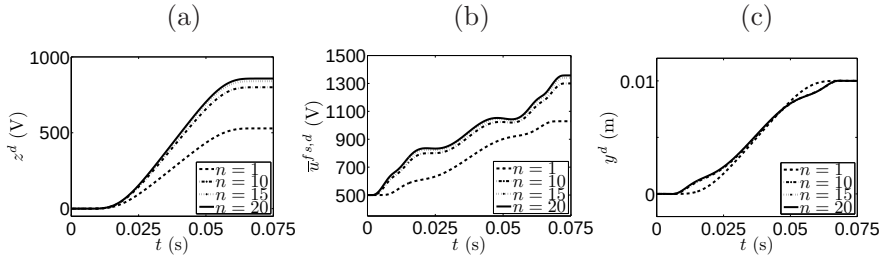

Figure 2. Convergence of flatness-based input and output parametrizations (34) and (25) for $n = 1, 10, 15, 20$. (a) Desired trajectory z^d for the flat output $z(t)$. (b) Input voltage $\overline{u}^{fs,d}(t) = u_0 - u^d(t)$ with $u_0 = 500$ V applied to the patch actuator located at the front side of the beam. (c) Output trajectory $y^d(t)$.

6. Conclusion and outlook

This contribution presents a systematic approach for motion planning and feedforward control design for a MFC-actuated flexible beam. As is shown in the companion paper [1], the inherent nonlinear hysteresis and creep behavior of the MFC actuators can be eliminated by the application of an appropriate hysteresis and creep compensator. From this it follows that a linear piezoelectric constitutive relation can be assumed for the motion planning and the feedforward control design. In this context, a flatness-based approach is proposed by introducing a flat output that parametrizes all states, the input and the output based on a finite-dimensional modal system representation. Numerical simulations show that the derived parametrizations converge with increasing system order of the finite-dimensional model. With the proposed solution of the motion planning problem the parametrization of the control input directly serves as an appropriate feedforward controller. Moreover, the applicability of this approach is verified by experimental results in the companion paper [1], where the realization of highly dynamic trajectories for the beam's tip deflection are presented. In order to deal, e.g., with exogenous disturbances, future research is devoted to augment the feedforward control with feedback control within the so-called two-degrees-of freedom control concept (see, e.g., [16]).

Post-print version of the article: J. Schröck, T. Meurer, and A. Kugi, "Control of a flexible beam actuated by macro-fiber composite patches: I. Modeling and feedforward trajectory control", *Smart Materials and Structures*, vol. 20, no. 015015, pp. 1–7, 2011. DOI: 10.1088/0964-1726/20/1/015015
The content of this post-print version is identical to the published paper but without the publisher's final layout or copy editing.

References

[1] J. Schröck, T. Meurer, and A. Kugi, "Flexible beam actuated by macro-fiber composite patches–Part II: Hysteresis and creep compensation, experimental results," *SIAM Smart Material and Structures*, 2010, submitted.

[2] H. Tzou and G. Anderson, *Intelligent Structural Systems*. Norwell, MA (USA): Kluwer, 1992.

[3] H. T. Banks, R. C. H. Smith, and Y. Wang, *Smart Material Structures: Modelling, Estimation and Control*. Paris (F): John Wiley & Sons, 1996.

[4] A. Preumont, *Vibration Control of Active Structures: An Introduction*, 2nd ed. Dortrecht (NL): Kluwer, 2002.

[5] H. Irschik, "A review on static and dynamic shape control of structures by piezoelectric actuation," *Eng. Struct.*, vol. 24, no. 1, pp. 5–11, 2002.

[6] J. Schröck, T. Meurer, and A. Kugi, "Motion planning for an adaptive wing structure with macro-fiber composite actuators," ser. SPIE Conference Series, vol. 7362, no. 1. Dresden (D): SPIE, May 4-6 2009, p. 73621H (11 pages).

[7] Z.-H. Luo, B.-Z. Guo, and O. Morgül, *Stability and Stabilization of Infinite Dimensional Systems with Applications*. London, Berlin, Heidelberg: Springer, 1999.

[8] M. Fliess, J. Lévine, P. Martin, and P. Rouchon, "Flatness and defect of non–linear systems: introductory theory and examples," *Int. J. Control*, vol. 61, pp. 1327–1361, 1995.

[9] M. Fliess and H. Mounier, "Tracking Control and π-freeness of infinite dimensional linear systems," in *Dynamical Systems, Control, Coding, Computer Vision: New trends, Interfaces, and Interplay*, G. Picci and D. Gilliam, Eds. Basel: Birkhäuser, 1999, pp. 45–68.

[10] P. Rouchon, "Motion planning, equivalence and, infinite dimensional systems," *Int. J. Appl. Math. Comp. Sc.*, vol. 11, pp. 165–188, 2001.

[11] J. Rudolph, *Flatness Based Control of Distributed Parameter Systems*, ser. Berichte aus der Steuerungs– und Regelungstechnik. Aachen: Shaker–Verlag, 2003.

[12] T. Meurer and M. Zeitz, "Feedforward and feedback tracking control of nonlinear diffusion-convection-reaction systems using summability methods," *Ind. Eng. Chem. Res.*, vol. 44, pp. 2532–2548, 2005.

[13] Y. Aoustin, M. Fliess, H. Mounier, P. Rouchon, and J. Rudolph, "Theory and practice in the motion planning and control of a flexible robot arm using Mikusiński operators," in *Proc. 5th IFAC Symposium on Robot Control*, Nantes (F), 1997, pp. 287–293.

[14] M. Fliess, H. Mounier, P. Rouchon, and J. Rudolph, "Systèmes linéaires sur les opérateurs de Mikusiński et commande d'une poutre flexible," *ESAIM Proc.*, vol. 2, pp. 183–193, 1997.

[15] J. Rudolph and F. Woittennek, "Flachheitsbasierte Randsteuerung von elastischen Balken mit Piezoaktuatoren," *at–Automatisierungstechnik*, vol. 50, pp. 412–421, 2002.

[16] T. Meurer, D. Thull, and A. Kugi, "Flatness–based tracking control of a piezoactuated Euler–Bernoulli beam with non–collocated output feedback: theory and experiments," *Int. J. Control*, vol. 81, no. 3, pp. 473–491, 2008.

[17] F. Woittennek and J. Rudolph, "Motion planning for a class of boundary controlled linear hyperbolic pde's involving finite distributed delays," *ESAIM Contr. Optim. Ca.*, vol. 9, pp. 419–435, 2003.

[18] J. Becker and T. Meurer, "Feedforward Tracking Control for Non–Uniform Timoshenko Beam Models: Combining Differential Flatness, Modal Analysis and FEM," *ZAMM*, vol. 87, no. 1, pp. 37–58, 2007.

[19] T. Meurer and A. Kugi, "Inversion-based transient shaping of piezo-actuated plate: Motion planning and feedforward control." Heidelberg (D): Proc. (CD-ROM) IFAC Symp. on Mechatr. Sys., Sep. 12-14, 2006, pp. 169–174.

[20] R. B. Williams, G. Park, D. J. Inman, and W. K. Wilkie, "An overview of composite actuators with piezoceramic fibers," *Proc. of 20th Int. Modal Analysis Conf.*, February 4-7 2002.

[21] Datasheet, http://www.smart-material.com.

Post-print version of the article: J. Schröck, T. Meurer, and A. Kugi, "Control of a flexible beam actuated by macro-fiber composite patches: I. Modeling and feedforward trajectory control", *Smart Materials and Structures*, vol. 20, no. 015015, pp. 1–7, 2011. DOI: 10.1088/0964-1726/20/1/015015

[22] W. Nowacki, *Dynamic Problems of Thermoelasticity*. Warszawa (PL): Noordhoff Int. Publ., PWN–Polish Scientific Publ., 1975.

[23] J. Wloka, *Partial Differential Equations*. Cambridge University Press, 1987.

[24] L. Meirovitch, *Dynamics and Control of Structures*. New York (USA): John Wiley & Sons, 1990.

[25] T. Meurer, J. Schröck, and A. Kugi, "Motion planning for a damped non-uniform Euler-Bernoulli beam," submitted to IEEE CDC 2010.

Post-print version of the article: J. Schröck, T. Meurer, and A. Kugi, "Control of a flexible beam actuated by macro-fiber composite patches: I. Modeling and feedforward trajectory control", *Smart Materials and Structures*, vol. 20, no. 015015, pp. 1–7, 2011. DOI: 10.1088/0964-1726/20/1/015015